Deep learning enabled wide-coverage high-resolution cardiac CT)

Tzu-Cheng Lee*[a], Jian Zhou[a], John Schuzer[a], Masakazu Matsuura[b], Takuya Nemoto[b], Hiroki Taguchi[b], Zhou Yu[a], Liang Cai[a]
[a] Canon Medical Research USA, Inc, 706 Deerpath Dr, IL 60061, USA; [b] CT Development Department, Canon Medical Systems Corporation, Tochigi 324-8550, Japan

ABSTRACT

Wide-coverage detector CT and ultra-high-resolution (UHR) detector CT are two important features for current cardiac imaging modalities. The former one enables the scanner to finish a whole heart image scan in one bed position; the latter one gives superior resolution in fine structures such as stenoses, calcifications, implemented stents, and small vessel boundaries. However, no commercially available scanner has both these features in one scanner as of today. Herein, we propose to use existing UHR-CT data to train a super resolution (SR) neural network and apply the network in a wide-coverage detector CT system. The purpose of the network is to enhance the system resolution performance and reduce the noise while maintaining its wide-coverage feature without additional hardware changes. Thirteen UHR-CT patient datasets and their simulated-normal-resolution pairs were used for training a 3D residual-block U-Net. The modulation transfer function (MTF) measured from Catphan phantom scans showed the proposed super-resolution aided deep learning-based reconstruction (SR-DLR) improved the MTF resolution by relative ~30% and ~10% as compared to filtered-back projection and model-based iterative reconstruction approaches. In real patient cases, the SR-DLR images show better noise texture and enhanced spatial resolution along with better aortic valve, stent, calcification, and soft tissue features as compared to other reconstruction approaches.

Keywords: super resolution, wide coverage detector, ultra-high resolution (UHR) CT, cardiac imaging

1. INTRODUCTION

Wide-coverage detector CT, such as the 16-cm coverage area of the Canon Aquilion ONE system, improves the ability to obtain high-quality images for routine cardiac and chest scans. It takes only one rotation to acquire a whole heart scan with less dose and great z-axis uniformity [1, 2]. Moreover, the superior time resolution from single bed position scans reduces possibility for motion artifact due to patient movement. Ultra-high resolution (UHR) CT, on the other hand, equipped with a finer size detector and smaller x-ray focal spot source, provides diagnostic images with two times the spatial resolution compared to current standard resolution CT (0.25 vs. 0.50 mm detector size at isocenter, Canon Aquilion Precision system for example). Several studies have shown improvements in tumor classification and staging [3, 4].

Ideally, a wide-coverage detector UHR-CT scanner is an advanced solution for cardiac imaging which offers better dose efficiency, spatial resolution and motion control at the same time. However, to the best of our knowledge, this ideal hardware system is currently not commercially available. Such a scanner may also have issues with image reconstruction, data transfer and processing times, or the inevitably higher cost. Therefore, an alternative approach for wide-coverage detector UHR-CT imaging is desirable.

Super-resolution (SR) technology aims at recovering high-resolution information from low-resolution images. Recent research has showed that deep convolution neural network-based (DCNN-based) SR approaches produce superior image quality along with processing speeds that compare with conventional methods [5, 6]. Nevertheless, none of references have shown the performance advantages of combining both wide-coverage and UHR-CT imaging on real clinical cases. In this work, we propose a super-resolution aided deep-learning based reconstruction (SR-DLR) framework for achieving near UHR image quality on a wide coverage detector CT system; with both UHR and wide coverage features without hardware modifications.

* elee@mru.medical.canon; phone 1 (847) 573- 6650; research.us.medical.canon

7th International Conference on Image Formation in X-Ray Computed Tomography,
edited by Joseph Webster Stayman, Proc. of SPIE Vol. 12304, 123041O
 · 0277-786X · doi: 10.1117/12.2647130

2. METHODS

The proposed super-resolution DCNN directly uses the high-resolution CT images acquired on our UHR CT scanner as the training target. In order to simulate lower resolution CT images for network training input, we perform data-domain downsampling and then the downsampled data are reconstructed to obtain the lower resolution or normal resolution (NR) input. Note that we do not recommend direct image-domain downsampling as it may introduce spatial interpolation artifacts and create potentially unrealistic CT images. Multiple dose levels from low to high are also considered in the simulations which allow the network to learn not only the resolution enhancement but also noise reduction in particular when the input dose is low. The optimized network is then applied on the real wide-coverage CT data for achieving the wide-coverage UHR CT-like image. The detailed workflow for training data preparation and network inference is shown in Figure 1. Currently the proposed DCNN is an image-domain super-resolution network but extension to data-domain super resolution is straightforward and will be investigated in our future work.

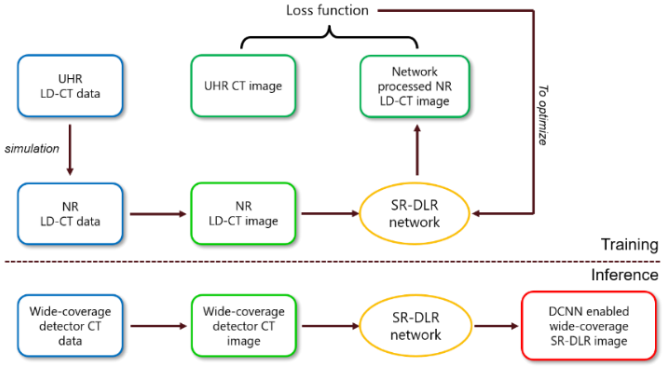

Figure 1 Training and inference processing flow of proposed DCNN enabled wide-coverage SR-DLR imaging.

2.1 Data Description

Thirteen high quality cardiac patient cases acquired from a UHR-CT system were used as the learning target. The acquisition energy and dose varied from 120 ~ 140 kVp and 150 ~ 190 mAs. Different reconstruction field of views and doses were applied and simulated for enriching data diversity. All target image dimensions reconstructed with model-based iterative reconstruction (MBIR) method were 1024x1024 pixels by 0.25 mm thickness. The acquired high-resolution data were first converted to the pre-log count domain, and then 2x2 data binning was applied to mimic the NR data. For more realistic data, additional white noise can be added at this step to compensate for the electronic noise. All simulated NR data were reconstructed with filtered-back projection (FBP) and standard ramp filter in the dimensions of 1024x1024 pixels and 0.25mm reconstruction pitch. The reconstructed SR-DLR images are compared with FBP and MBIR images. For quantitative comparison, the Catphan-600 phantom with different modules were used to evaluate the resolution improvement in terms of MTF (modulation transfer function) and line pairs (lp/cm) analysis. One true UHR-CT patient data (140kVp, 164mAs, 150mm FOV, 0.25mm reconstruction pitch) also used for comparison as shown in Figure 4. NR simulation process as stated in previous publication [7]. Another three real normal resolution (NR-CT) patient scans (see Table 1) were reconstructed to test the image quality through visual inspection. All images in result section reconstructed in default 512x512 pixels (SR-DLR in 1024x1024 pixels) with 240-mm field of view and 0.25 mm reconstruction pitch.

Table 1 Dose information for three representative patient cases

Patient	kVp	mAs	CTDI(mGy)	Remarks
A	100	63.3	2.5	Low-dose
B	120	159.5	9.4	Stent
C	120	206.3	14.3	High calcium

2.2 Network Architecture, Training and Implementation

The SR-DLR network adopts the U-NET structure with residual 3D convolutional blocks as basic building units, which enables deep structure without gradient vanishing and maintains proper receptive field for capturing large spatial features in the image (see Figure 2) [8, 9]. In network training we used small patches of size 32x128x128. Data argumentation such as patch flipping were also performed during the training. The training was mainly conducted using the TensorFlow-Keras

(ver. 2.3) framework with Nvidia Titan RTX GPUs for acceleration. We chose the ADAM optimizer and the mean absolute error loss function. A total 200 epochs were run for effective convergence.

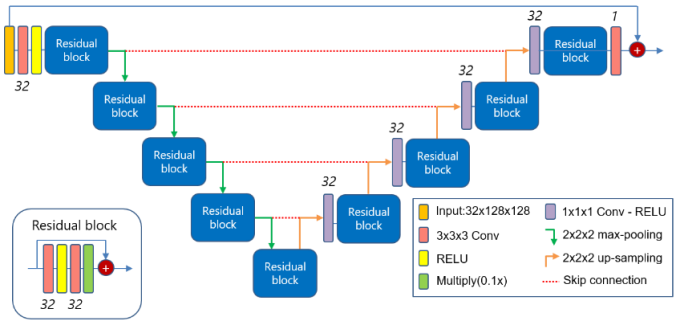

Figure 2 The proposed SR-DLR network which includes a 3D-UNET structure with residual blocks. The number beside the convolutional layer represents the number of filters.

3. RESULTS

3.1 Quantitative Evaluation

SR-DLR imaging shows superior 200mm FOV MTF performance as compared to FBP and MBIR reconstruction among all three materials. For low-contrast polystyrene (~-30HU), SR-DLR improves 10%-MTF to 1.04 lp/mm compares to 0.77 in FBP and 0.80 in MBIR. For mid-contrast Delrin (~330HU), 10%-MTF in SR-DLR is 1.15 lp/mm compares to 0.86 in FBP and 0.91 in MBIR. For high-contrast Teflon (~900HU), 10%-MTF in SR-DLR is 1.24 lp/mm compares to 0.86 in FBP and 1.11 in MBIR. (see Figure 3).

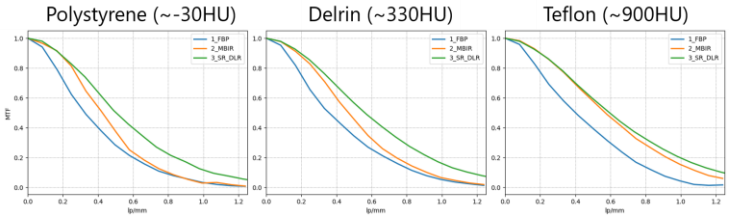

Figure 3 Modulation transfer function measurement as a function of line pair per millimeter with three different representative materials (polystyrene, Delrin and Teflon) in standard CATPHAN phantom (CTP404 module). Three different reconstruction methods (FBP in blue, MBIR in orange and proposed SR-DLR in green) listed from 0 to 1.25 lp/mm for comparison.

3.2 Comparison with True UHR-CT Images

Figure 4 compares the SR-DLR image to the closest-ground-truth image (e.g. true UHR-CT MBIR image) so that the resolution performance can be examined. The simulated-NR SR-DLR phantom image has better bar resolution compared to the FBP image (~9 lp/cm vs. ~8 lp/cm). The image contrast as well as the bar intensity of SR-DLR is also closer to the ground truth image compared to the FBP reconstruction. The simulated NR SR-DLR patient image shows better resolution in stent and higher contrast in soft tissue compares to the FBP image. No artificial feature created when we compare NR SR-DLR to the true UHR-CT patient image.

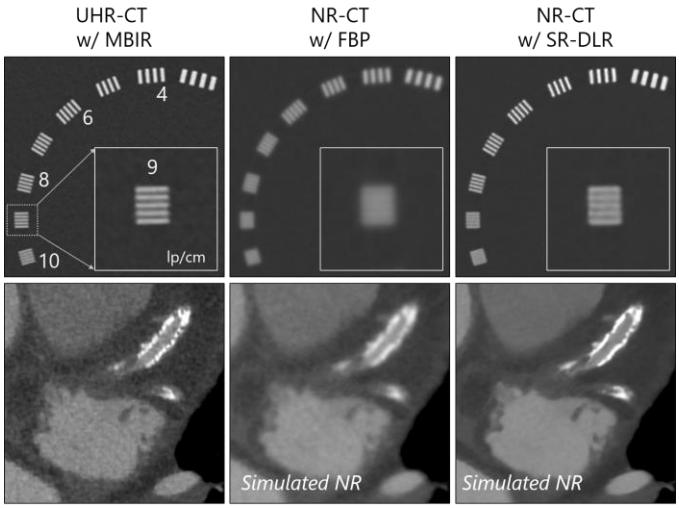

Figure 4 Resolution phantom module (CTP528 module) and patient examples. Upper row: two reconstruction methods with normal resolution (NR) data to the true UHR-CT MBIR image. The 9 lp/cm contrast bars are zoomed in the bottom-right small image. Window level and width: 1000 and 3000 HU. Lower row: two simulated NR data for FBP and SR-DLR reconstructions to the true UHR-CT MBIR patient image. Window level and width: 350 and 1500 HU

3.3 Compare SR-DLR Image to Other Reconstructions

In Figure 5, we are able to see the noise and resolution differences when comparing SR-DLR images to FBP and MBIR reconstructions. Patient (A) images shows that the SR-DLR image has better resolution for the aortic valve and better contrast of small vessels. Patient (B) images further show cleaner microstructure of the implanted stent. Patient case (C) shows the SR-DLR image has sharper calcification contrast and boundaries compared to other two reconstruction methods. In addition, SR-DLR has lowest noise and sharpest soft tissue boundaries among these three methods.

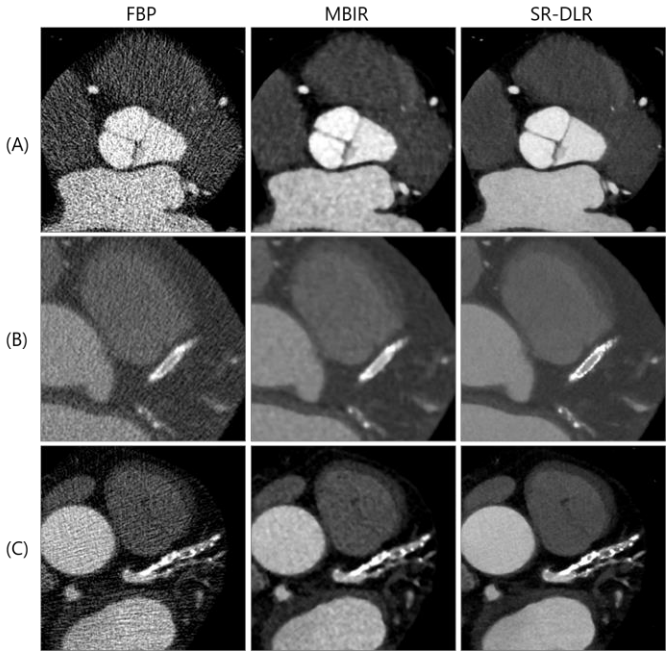

Figure 5 Three representative patient cases (case A: aortic valve; case B: stent; case C: calcium) with three different reconstruction methods. Window level and width for case A and C: 300 and 800 HU; for case B: 350 and 1500 HU.

4. CONCLUSIONS

Testing on quantitative phantom data and clinical patient data shows that SR-DLR is a promising approach for enhancing resolution and suppressing noise. In summary, the proposed method has advantages over prior approaches: compared to current wide-coverage detector CT imaging, the proposed method improves resolution and noise performance; this improvement is gained from the UHR-CT trained network with finer reconstructed pixel sizes. Compared to UHR-CT system imaging, this method has wider-detector coverage data as the input, which benefits dose efficiency, image uniformity, and motion management. The larger acquisition detector pixel size from wide-coverage CT also benefits noise performance. Compared to a hypothetical wide-coverage UHR-CT system, the SR-DLR method has substantially lower cost and much less image processing complexity from both hardware and software perspectives.

ACKNOWLEDGMENT

Authors would like to thank Dr. Marcus Chen, M.D. and his group at Cardiovascular CT Program of NHLBI, NIH for data collection and their insightful clinical feedbacks.

REFERENCES

[1] Lewis M, *et. al*, "Selecting a CT scanner for cardiac imaging: the heart of the matter" *BJR* 2016 (89):376

[2] Annoni A, *et. al*, "CT angiography prior to TAVI procedure using third-generation scanner with wide volume coverage: feasibility, renal safety and diagnostic accuracy for coronary tree" *BJR* 2018 (91):196

[3] Yanagawa M, *et. al*, "Subjective and objective comparisons of image quality between ultra-high-resolution CT and conventional area detector CT in phantoms and cadaveric human lungs" *European Radiology* 2018 (28):5060

[4] Hata A, *et. al*, "Effect of matrix size on the image quality of ultra-high-resolution CT of the lung" *Acad Radiol.* 2018 (25):869

[5] Yu, H. *et. al*,"Computed tomography super-resolution using convolutional neural networks," *2017 IEEE International Conference on Image Processing (ICIP)* 2017

[6] Umehara, K. *et. al*, "Application of super-resolution convolutional neural network for enhancing image resolution in chest CT," *J Digit Imaging* 2018; 31(4): 441-450

[7] Hernandez, A. et. al, "Validation of synthesized normal-resolution image data generated from high-resolution acquisitions on a commercial CT scanner" *Medical Physics*, 2020; 47(10):4776

[8] Lim, B. et. al, "Enhanced deep residual networks for single image super-resolution" 2017, arXiv:1707.02921

[9] Milletari, F. et. al, "V-Net: fully convolutional neural networks for volumetric medical image segmentation," 2016, arXiv:1606.04797